Multiexponential Diffusion Measurements of Varying Densities of Astrocytoma Cells

P. R. Jackson[1], R. G. Henry[2], and T. R. McKnight[2]

[1]Joint Graduate Group in Bioengineering, University of California, Berkeley and San Francisco, San Francisco, CA, United States, [2]Department of Radiology, University of California, San Francisco, San Francisco, CA, United States

Introduction

A primary histologic feature that indicates malignant progression of glioma is an increase in cell density. Several studies have shown that the monoexponential apparent diffusion coefficient appears to be linked to cell density [1]. Other studies have used biexponential [2] or unconstrained multiexponential models[3] to extract multiple components from cells and tissue. Because of the complex structure of the cellular and extracellular components that comprise tissue, it is unlikely that the monoexponential model reflects the totality of the diffusive processes in tumors. In order to tease out which diffusive properties are directly linked to cell density, we created a simple model for tissue using varying densities of astrocytoma cells to better understand the effects of cell density on diffusion coefficients.

Methods

SAMPLE PREP: Cultured genetically engineered astrocytoma cells [4] were trypsinized, washed in D_2O based Phosphate Buffered Saline (D-PBS), and centrifuged at 400×g at 5°C. Two percent (w/v) low melting point agarose (Sea Prep, Lonza, Basel, Switzerland) was made with D-PBS and TSP/D_2O. Cells and agarose were mixed to create samples that were 0%, 25%, 50%, 75% and 100% cells (N=3 each). The cell and agarose mixtures were loaded into a dual-open-ended 5mm NMR tube with susceptibility matched plugs (New Era, Vineland, NJ). Each sample was placed on ice and allowed to gel for at least 2 hours prior to performing NMR measurements.

NMR MEASUREMENTS: All NMR experiments were performed at 10°C on a 500MHz Varian spectrometer equipped with 60G/cm z-gradients. Diffusion experiments were performed in the z-direction using the DgcsteSL sequence: δ = 3ms, Δ = 50ms, TE=6ms, TR=7s, NEX=1, spin lock = 2ms. Thirty-two linearly spaced b-values were used: for 100%, 75%, and 50% samples b=10 to 9000s/mm^2; for 25% samples b=10 to 2800s/mm^2; and for 0% samples b=10 to 1095s/mm^2.

DATA ANALYSIS: The water peak heights were measured at 4.9ppm using ACD (Toronto, Canada) and were used to construct diffusion decay curves. The resulting exponentials were analyzed using monoexponential (ME), biexponential (BE), Non-Negative Least Squares (NNLS) [5] algorithms in MATLAB (MathWorks, Natick, MA). The general fit equation was

$$S/S_0 = \sum_{a=1}^{n} f_a e^{-bD_a}$$

where S/S_0 is the normalized signal intensity, D is the diffusion coefficient, f_a is the fraction of signal associated with a particular D, b is the diffusion weighting, and n is the number of components. For monoexponential fits n=1, and for biexponential fits n=2 . The variable n was not assigned *a priori* for NNLS , but was one of the fit parameters. Only components that contributed more than 10% to the signal ($f_a > 0.10$) were assumed to be true components rather than errors arising from noise in the model. Spearman Rank correlation with a significance level of $p \leq 0.01$ was used to detect correlations with cellularity while controlling for multiple comparisons.

Results

The diffusivity from the ME fit (Figure 1, blue) decreased with increasing cell volume ($p<0.001$). The BE analysis successfully fit two components (Figure 1, green and red) for 50%, 75%, and 100% cells, but only detected one component for 0% and 25% samples. In Figure 1, the fast diffusion coefficient (green) decreased with increasing cell density ($p<0.001$), while slow diffusion (red) remained constant ($p=0.22$). Figure 2 shows that, the signal fraction for fast diffusion (green) decreased ($p<0.001$) and the slow diffusion fraction increased ($p<0.001$) with increasing cellularity.

Tthe NNLS fit (Figure 3) one component for 0% and 25% cells, three components for 50% and 75% cells, and two components for 100% cells. The slow ($p=0.32$) diffusion coefficients stayed relatively constant across all samples, while the fast ($p=0.05$) tended to decrease with increasing cellularity. The intermediate coefficient (yellow) decreased with increasing cell density ($p=0.01$). Figure 4 shows that the fast signal fraction decreased ($p<0.001$), the slow fraction increased ($p=0.001$) and the intermediate fraction remained constant ($p=0.10$).

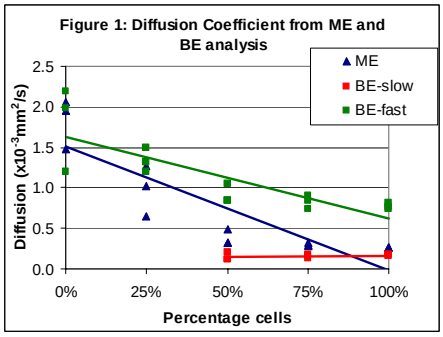

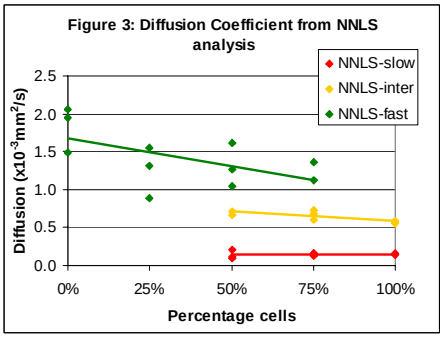

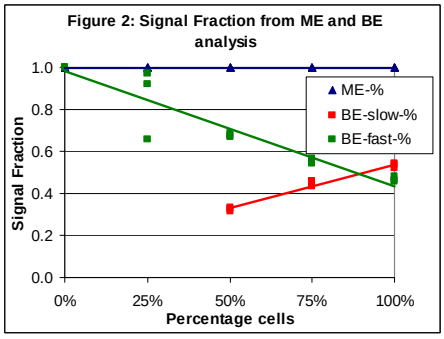

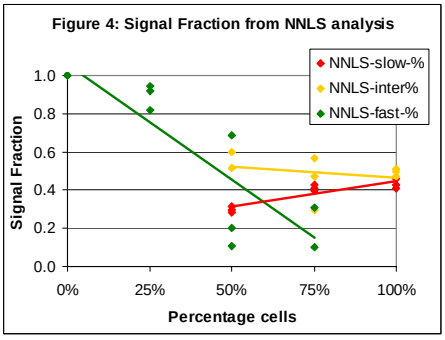

Discussion

As expected, all three methods detected a single diffusion component in the homogenous 0% sample, which is pure agarose. The 25% cell samples were also found to have one component despite the presence of cells; however the diffusion coefficient was reduced.

We were able identify two components with BE analysis for the 50%, 75%, and 100% samples, and the introduction of cells contributed a slower diffusion component. The fractions of both components changed with cell density but the coefficients remained constant.

Using the unconstrained NNLS analysis that did not impose a fixed number of components on the model, we were able to identify three components for the 50% and 75% samples and two components (intermediate and slow) for the 100% samples. The 0% (pure agar) samples only featured a fast diffusion component. The slow and fast diffusion coefficients (Figure 3) were not significantly correlated with cell density; however, the intermediate component did have an inverse relationship with cell density.

This data suggests that the slow component appeared to be associated with the cells. Further, the monoexponential diffusion was dominated by the fast diffusion component. Interestingly, the fast diffusion tracked well with agar presence.

For future studies, we will further test the relationships we saw here by changing the diffusive properties of the agar (e.g. concentration) and the cells (e.g. volume).

Acknowledgements: Dr. John Kurhanewicz

References: 1. Sugahara, T., et al., J Magn Reson Imaging, 1999. **9**(1): p. 53-60., 2. Grant, S.C., et al., Magn Reson Med, 2001. **46**(6): p. 1107-12. 3. Ronen, I., et al., Magn Reson Imaging, 2006. **24**(4): p. 425-31. 4. Sonoda, Y., et al., Cancer Res, 2001. **61**(13): p. 4956-60. 5. Lawson, C.L. and R.J. Hanson, 1974, Englewood Cliffs, N.J.: Prentice-Hall. xii, 340.